Role of the WNK-activated SPAK kinase in regulating blood pressure

Fatema H. Rafiqi[1], Annie Mercier Zuber[2][†], Mark Glover[2][†], Ciaran Richardson[1], Stewart Fleming[3], Sofija Jovanović[4], Aleksandar Jovanović[4], Kevin M. O'Shaughnessy[2]*, Dario R. Alessi[1]*

Mutations within the with-no-K(Lys) (WNK) kinases cause Gordon's syndrome characterized by hypertension and hyperkalaemia. WNK kinases phosphorylate and activate the STE20/SPS1-related proline/alanine-rich kinase (SPAK) protein kinase, which phosphorylates and stimulates the key Na^+:Cl^- cotransporter (NCC) and Na^+:K^+:$2Cl^-$ cotransporters (NKCC2) cotransporters that control salt reabsorption in the kidney. To define the importance of this pathway in regulating blood pressure, we generated knock-in mice in which SPAK cannot be activated by WNKs. The SPAK knock-in animals are viable, but display significantly reduced blood pressure that was salt-dependent. These animals also have markedly reduced phosphorylation of NCC and NKCC2 cotransporters at the residues phosphorylated by SPAK. This was also accompanied by a reduction in the expression of NCC and NKCC2 protein without changes in messenger RNA (mRNA) levels. On a normal Na^+-diet, the SPAK knock-in mice were normokalaemic, but developed mild hypokalaemia when the renin–angiotensin system was activated by a low Na^+-diet. These observations establish that SPAK plays an important role in controlling blood pressure in mammals. Our results imply that SPAK inhibitors would be effective at reducing blood pressure by lowering phosphorylation as well as expression of NCC and NKCC2. See accompanying Closeup by Maria Castañeda-Bueno and Gerald Gamba (DOI 10.1002/emmm.200900059).

INTRODUCTION

Since the discovery that mutations within human with-no-K(Lys) kinase-1 (WNK1) and WNK4 genes cause a form of hypertension and hyperkalemia termed Gordon's syndrome (pseudohypoaldosteronism type II, PHAII) (Flatman, 2008; Kahle et al, 2008; Wilson et al, 2001), these enzymes have taken centre stage in research aimed at understanding signal transduction networks that regulate ion homeostasis and blood pressure. In the case of WNK1, the mutations lie within intronic regions and lead to increased enzyme expression and hypertension (Wilson et al, 2001). Consistent with this, heterozygous $WNK1^{+/-}$ knock-out mice have lower blood pressure (Zambrowicz et al, 2003). Mutations in WNK4 that cause PHAII alter amino acid sequences within the non-catalytic C-terminal moiety of the enzyme (Golbang et al, 2005; Wilson et al, 2001).

The cellular activity of the WNK kinases is stimulated by either hyperosmotic or hypotonic low-chloride conditions (Lenertz et al, 2005; Zagorska et al, 2007). The best-characterized WNK substrates comprise the STE20/SPS1-related proline/alanine-rich kinase (SPAK) and oxidative stress-responsive kinase 1 (OSR1), which are activated following their phosphorylation by WNK1 or WNK4 (Delpire & Gagnon, 2008; Richardson & Alessi, 2008; Vitari et al, 2005). These WNK isoforms interact directly with SPAK as well as OSR1 and phosphorylate these enzymes at two conserved

(1) MRC Protein Phosphorylation Unit, MSI/WTB Complex, University of Dundee, Dundee, Scotland, UK.
(2) Clinical Pharmacology Unit, Department of Medicine, University of Cambridge, Cambridge, UK.
(3) Division of Molecular Pathology, Ninewells Hospital and Medical School, University of Dundee, Dundee, Scotland, UK.
(4) Division of Medical Sciences, Centre for Cardiovascular and Lung Biology, Ninewells Hospital and Medical School, University of Dundee, Dundee, Scotland, UK.

*Corresponding author: Tel: +44 1382 385 602; Fax: +44 1382 223 778; E-mail: kmo22@medschl.cam.ac.uk; d.r.alessi@dundee.ac.uk
†AMZ and MG contributed equally to this manuscript.

residues, namely the T-loop Thr residue (Thr243 in mouse SPAK) and at a Ser residue in the S-motif (Ser383 in mouse SPAK) (reviewed in Richardson et al, 2008). T-loop phosphorylation triggers activation of SPAK and OSR1, as its mutation to Ala prevents activation (Vitari et al, 2005; Zagorska et al, 2007). The role of S-motif phosphorylation is unclear, as its mutation does not affect activation (Vitari et al, 2005; Zagorska et al, 2007).

The only substrates of SPAK and OSR1 kinases that have been identified thus far are members of the electroneutral cation-coupled chloride cotransporters (SLC12), including the $Na^+:Cl^-$ cotransporter (NCC) and the $Na^+:K^+:2Cl^-$ cotransporters (NKCC1 and NKCC2), that are known targets for the blood-pressure-lowering thiazide diuretic and loop diuretic drugs (Flatman, 2008; Gamba, 2009; Ko & Hoover, 2009). These cotransporters play vital roles in regulating ion transport and ion homeostasis. Hence, loss-of-function-mutations in NCC and NKCC2 lead respectively to the salt wasting Gitelman's and Bartter's syndromes of hypotension and hypokalaemia underlining the obligate nature of these transporters for renal electrolyte transport (Simon et al, 1996a, b). Both SPAK and OSR1 interact and phosphorylate SLC12 ion cotransporters at a cluster of conserved Thr residues located at their N-terminal cytosolic domain (reviewed in Ko & Hoover, 2009; Richardson & Alessi, 2008). This phosphorylation stimulates the ability of the ion cotransporters to transport ions across the plasma membrane. The finding that the mutation of a key SPAK/OSR1 phosphorylation site on NCC (Thr60) (Pacheco-Alvarez et al, 2006; Richardson et al, 2008), causes Gitelman's syndrome (Shao et al, 2008) also emphasizes the importance of SPAK/OSR1 in regulating the activity of NCC. Furthermore, a recent genome-wide association study revealed that intronic single nucleotide polymorphisms (SNPs) within the human SPAK gene increase blood pressure by enhancing expression of SPAK in the kidney and suggests that SPAK may also regulate blood pressure within the general population (Wang et al, 2009).

Although these observations suggest that the WNK kinases regulate blood pressure through their ability to control the activity of the SPAK/OSR1 and SLC12 cotransporters, numerous reports have concluded that WNK isoforms exert functions independent of SPAK/OSR1 *in vitro*. For example, WNK isoforms have been reported to interact, phosphorylate and/or control the function of many other enzymes including the serum and glucocorticoid induced kinase, the epithelial sodium channel, the renal outer medullary potassium channel, the transient receptor potential vanilloid-4/5 calcium channel, the cystic fibrosis transmembrane conductance regulator, claudin isoforms, synaptotagmin 2 and the chloride/base exchanger SLC26A6 (reviewed in Huang et al, 2007; Kahle et al, 2008). WNK1 was also reported to activate the ERK5 protein kinase (Xu et al, 2004) and modulate TGFβ-Smad signalling (Lee et al, 2007). Thus, the relative importance of SPAK/OSR1-dependent and independent pathways in controlling the ability of WNK isoforms to regulate blood pressure *in vivo* is not clear.

To investigate the role of SPAK in controlling the phosphorylation of SLC12 family cotransporters and regulating blood pressure, we generated knock-in mice in which SPAK is still expressed but cannot be activated by WNK isoforms. Most importantly, we demonstrate that preventing SPAK activation by WNK kinases significantly reduced blood pressure by suppressing expression and phosphorylation of the NCC and NKCC2 ion cotransporters. These observations provide genetic evidence that the ability of WNK kinases to influence and control blood pressure in mammals is mediated at least in part though SPAK and suggest that SPAK may be a novel target for anti-hypertensive drug therapy.

RESULTS

Generation of knock-in mice

Knock-in mice in which the T-loop Thr residue in SPAK (Thr243) and OSR1 (Thr185) were mutated to Ala to prevent activation by WNK isoforms were generated as described in Supporting Information Fig 1. Single homozygous SPAK$^{243A/243A}$ mice were born at the expected Mendelian frequency and did not display any overt phenotype (Table S1). In contrast, no homozygous SPAK$^{+/+}$OSR1$^{185A/185A}$ mice were born in crosses of heterozygous SPAK$^{+/+}$OSR1$^{185A/+}$ animals (Table S1). Analysis of embryos indicated that SPAK$^{+/+}$OSR1$^{185A/185A}$ fetuses were detected up to day 17.5 of embryogenesis, suggesting that embryos perished late in development (Table S1). For the purpose of this study we focused our subsequent analysis on the viable SPAK knock-in animals. It should be noted that the SPAK knock-in mice were generated and maintained on an inbred C57BL/6J background. C57BL/6J mice have only a single renin isoform, in contrast to other inbred strains such as 129/Sv that possess two highly related renin isoforms (Pradervand et al, 1999; Sigmund & Gross, 1991). We utilized quantitative real-time PCR to confirm that the heterozygous and homozygous SPAK knock-in animals utilized in this study possess only a single renin isoform, in contrast to 129/Sv mice that have two renin isoforms (Fig S2).

Characterization of SPAK and OSR1 expression and activity in mice

To analyse SPAK and OSR1, we generated new antibodies capable of specifically immunoblotting and immunoprecipitating SPAK or OSR1 (Fig S3A and B). Immunoprecipitates of endogenous SPAK or OSR1 derived from mouse kidney or testis were analysed by mass spectroscopy. This confirmed that the SPAK antibody immunoprecipitated SPAK, but not OSR1 and that the OSR1 antibody only immunoprecipitated OSR1 (Fig S3C and D). This analysis also revealed the presence of several distinct forms of SPAK (Fig S3C), but only one species of OSR1 (Fig S3D). The coverage of tryptic peptides identified from the different forms of SPAK by mass spectrometry are summarized in Supporting Information Fig 3E.

Although OSR1 was expressed at similar levels in all tissues studied, SPAK expression was more variable and was most abundant in the testis, spleen, heart as well as brain and expressed at lower levels in other tissues analysed (kidney, lung, liver and skeletal muscle) (Fig 1A). Importantly, despite
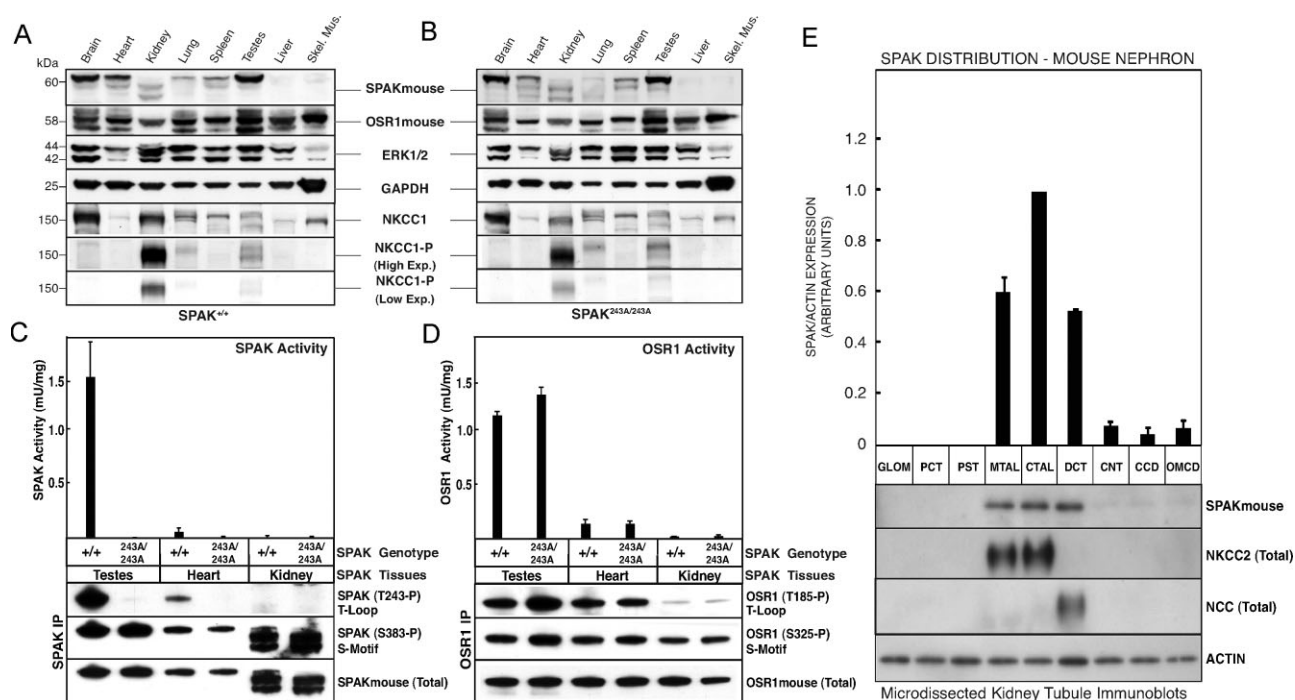
Figure 1. Expression and activity of SPAK and OSR1 in the tissues of wild type and SPAK$^{243A/243A}$ mice.

A, B. Expression of SPAK and OSR1 in tissues from wild type and knock-in mice. The indicated tissue extracts (40 μg protein) from wild type (A) and SPAK$^{243A/243A}$ mice (B) were subjected to immunoblot analysis with the specified antibodies. Immunoblots in (A) and (B) were run in parallel and exposed for the same amount of time to ensure that signal intensities can be directly compared. Similar results were obtained in three separate experiments.

C. Activity of SPAK in wild type and knock-in mouse tissues. SPAK was immunoprecipitated from the testis, heart and kidney lysates from wild type and SPAK$^{243A/243A}$ mice using the SPAK mouse peptide antibody. The immunoprecipitates were subjected to activity measurements using the CATCHtide peptide substrate (Vitari et al, 2006). A fraction of the immunoprecipitates was also subjected to immunoblot assay with the indicated antibodies.

D. Activity of OSR1 in wild type and knock-in mouse tissues. Same as (C) except OSR1 was immunoprecipitated from the wild type and SPAK$^{243A/243A}$ mouse extracts using the OSR1 mouse peptide antibody. The activity assay results are presented as mU/mg ± SEM. Similar results were obtained in three independent experiments.

E. Expression of SPAK, NKCC2 and NCC in microdissected kidney tubules. Kidney tissue was microdissected from wild type (WT) mice. Parts of the nephron isolated were glomerulus (Glom), proximal convoluted tubule (PCT), proximal straight tubule (PST), medullary thick ascending loop of Henle (MTAL), cortical thick ascending loop of Henle (CTAL), distal convoluted tubule (DCT), connecting tubule (CNT), cortical collecting duct (CCD) and outer medullary collecting duct (OMCD). These were subjected to immunoblotting analysis with the indicated antibodies. Stripping technique was used to clean the membrane between each antibody. Expression quantification of SPAK/actin is presented as arbitrary units ± SEM from three independent experiments.

the relatively low level of expression in the kidney, its distribution was very restricted within the mouse nephron. Highest levels were present in the medullary and cortical thick ascending loop of Henle (MTAL and CTAL) and the distal convoluted tubule (DCT) (Fig 1E). SPAK therefore colocalizes with NKCC2 and NCC in the distal nephron (Fig 1E). The faster migrating species of SPAK was most prominent in the kidney (Fig 1A). Importantly, levels of SPAK and OSR1 were similar in tissues derived from wild type and SPAK$^{243A/243A}$ knock-in mice, demonstrating that the Thr243Ala mutation does not influence protein expression/stability (Fig 1A and B). SPAK and OSR1 were immunoprecipitated from tissue extracts derived from wild type and SPAK$^{243A/243A}$ knock-in mice and their kinase activity as well as their phosphorylation at their T-loop and S-motif were analysed (Fig 1C and D). SPAK activity and T-loop phosphorylation was highest in the testis and heart of wild type mice (Fig 1C). In the kidney, SPAK was significantly

phosphorylated on its S-motif but not at its T-loop residue, most likely accounting for the low SPAK activity observed. Crucially, SPAK immunoprecipitated from the testis or heart of SPAK$^{243A/243A}$ mice was devoid of kinase activity and possessed no T-loop (Thr243) phosphorylation, while phosphorylation of the S-motif (Ser383) was unaffected (Fig 1C). This confirms that the knock-in mutation does indeed ablate SPAK activity. We found that OSR1 was similarly active and phosphorylated in the testis, heart and kidney of wild type and SPAK$^{243A/243A}$ knock-in mice (Fig 1D). This establishes that ablation of SPAK activity does not affect expression or activity of OSR1.

Reduced blood pressure in SPAK knock-in mice

Employing a real-time radiotelemetry approach, we assessed male wild type and SPAK$^{243A/243A}$ knock-in mice on a normal Na^{+}-diet (0.3% w/w) through continuous undisturbed monitoring of locomotor activity, heart rate and blood pressure
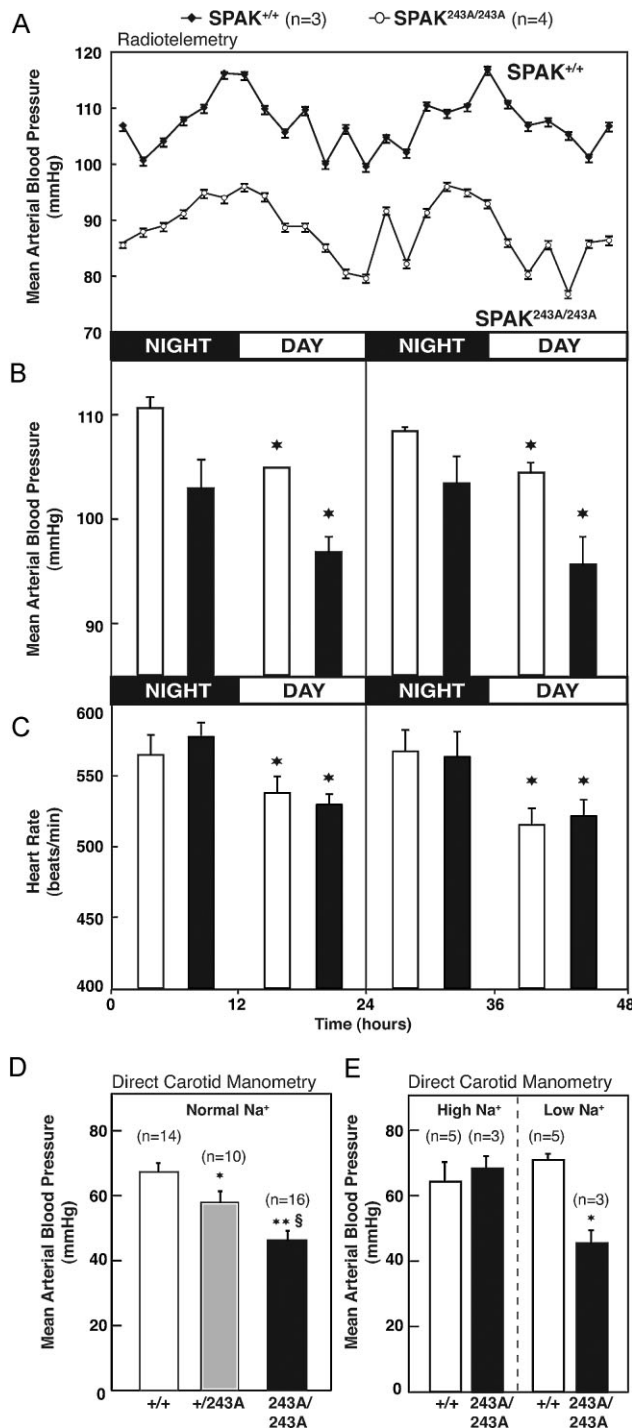
Figure 2. Mean arterial blood pressure is reduced in SPAK$^{243A/243A}$ mice.
Employing a real-time radiotelemetry approach, we assessed male wild type and SPAK$^{243A/243A}$ knock-in mice fed a normal (0.3% Na$^+$) salt diet through continuous undisturbed monitoring of blood pressure (**A** and **B**) and heart rate (**C**).

A. Time course of mean arterial blood pressure in wild type and knock-in mice over 48h period. In the line graph, each point represents the mean ± SEM of 720 mean arterial blood pressure averages recorded every 10 s. Each bar represents the mean ± SEM. $^*p < 0.01$ when night and day of the same phenotype were compared.

B. Diurnal rhythm of mean arterial blood pressure in wild type and knock-in mice.

C. Diurnal rhythm of heart rate in wild type and knock-in mice. 12 h averages (night or day as depicted) of blood pressure and heart rate measured over two successive days. $^*p < 0.01$ when night and day of the same phenotype were compared. Each bar represents the mean ± SEM.

D. Mean arterial BP (mm Hg) measured in the carotid artery of anaesthetized mice that had been fed a normal (0.3% Na$^+$) salt diet. $^*p < 0.05$, $^{**}p < 0.0001$ versus wild type, SPAK$^{+/+}$, $^§p < 0.01$ versus heterozygotes, SPAK$^{+/243A}$.

E. Mean arterial BP (mmHg) measured in the carotid artery of anaesthetized mice fed for 2 weeks on either high (3% Na$^+$) or low (0.03% Na$^+$) salt diets. $^*p < 0.001$ versus wild type, SPAK$^{+/+}$.
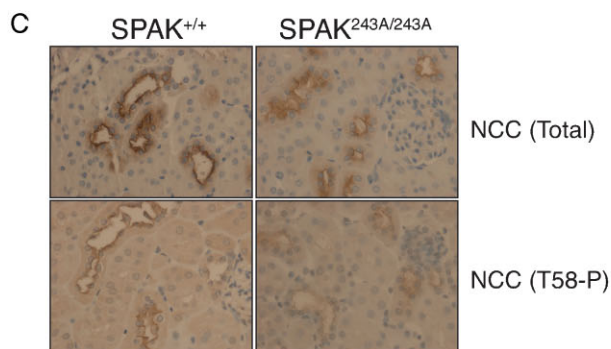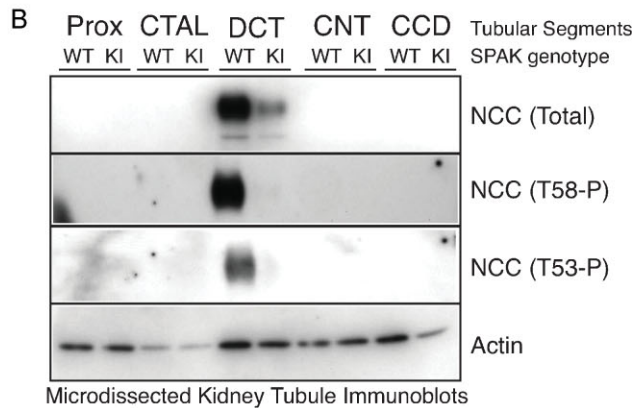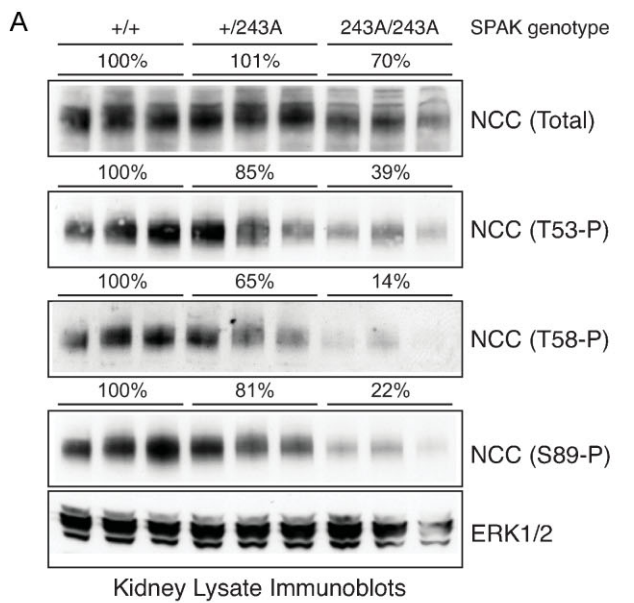
an intermediate reduction of blood pressure (Fig 2D). The difference in mean arterial blood pressure between wild type and SPAK$^{243A/243A}$ knock-in mice was preserved over the course of both day and night, with higher blood pressure measured at night when animals are more active (Fig 2A and B). Furthermore, the hypotensive phenotype of SPAK$^{243A/243A}$ mice was abolished by feeding mice a high (3% Na$^+$) but not augmented by a low (0.03% Na$^+$) salt diet (Fig 2E).

Reduced phosphorylation and expression of NCC in kidney of SPAK knock-in mice

We next investigated the impact of ablating SPAK activity on expression and phosphorylation of the NCC ion cotransporters in mouse kidney. Immunoblotting of kidney extracts demonstrated that NCC protein was reduced ∼30% in SPAK$^{243A/243A}$ knock-in animals. The heterozygous SPAK$^{243A/+}$ mice express similar levels of NCC as the wild type (Fig 3A). Quantitative PCR analysis revealed that NCC messenger RNA (mRNA) levels were similar in the kidney of wild type and SPAK$^{243A/243A}$ mice (Fig S4).

Employing the previously characterized phosphospecific antibodies, we analysed the phosphorylation of mouse NCC at residues Thr53 and Thr58 (equivalent to Thr55 and Thr60 in human NCC) that are directly phosphorylated by SPAK and OSR1 (Richardson et al, 2008). We also studied phosphorylation of Ser89 (equivalent to Ser91 in human NCC), a residue whose phosphorylation may also be controlled by SPAK/OSR1 (Richardson et al, 2008). We observed that NCC was significantly phosphorylated at Thr53, Thr58 and Ser89 in kidney extracts derived from wild type animals (Fig 3A). Phosphorylation of NCC at these residues was only moderately reduced in heterozygous SPAK$^{243A/+}$ animals. However, in SPAK$^{243A/243A}$ mice, we observed ∼2.6-fold (Thr53), 7.2-fold (Thr58-crucial activating residue) and 4.6-fold (Ser89) reduction of NCC phosphorylation (Fig 3A).

(Fig 2A–C). The heart rate (Fig 2C) and locomotor activity (data not shown) of both wild type and SPAK$^{243A/243A}$ knock-in mice demonstrated a normal circadian rhythm with no significant difference between the genotypes. However, the mean arterial BP was significantly lower in the SPAK$^{243A/243A}$ mice (Fig 2A and B). This difference in BP was confirmed when the carotid artery pressure was measured directly via manometry in a larger sample of anaesthetized mice with the heterozygotes showing

Figure 3. Reduced expression and phosphorylation of NCC in SPAK[243A/243A] mice.

A. Expression and phosphorylation of NCC in wild type and knock-in mouse kidney. Kidney extract derived from the indicated mice were subjected to immunoblot analysis with the specified NCC antibodies. Each sample is derived from a separate littermate animal. Band intensities were quantified using Li-Cor Odyssey and the results are presented relative to the wild type (100%). This study has been repeated over six times each with kidney extracts derived from different animals on each occasion with consistent results.

B. Expression and phosphorylation of NCC in wild type and knockin microdissected kidney tubules. Kidney tissue was microdissected from wild type (WT) or SPAK[243A243A] (KI) littermate mice. Tubular segments isolated are proximal tubule (PCT), cortical portions of the thick ascending limb (CTAL), distal convoluted tubule (DCT), connecting tubule (CNT) and cortical and outer medullary portions of the collecting duct (CCD). These were subjected to immunoblotting analysis with the indicated antibodies.

C. Immunohistochemical analysis of the expression and phosphorylation of NCC in wild type and knock-in mouse kidney. Immunohistochemical staining of whole kidney sections derived from the indicated mice probed with NCC total and phospho (Thr58) antibodies and visualized at a magnification of ×40.

between the two genotypes. Apical staining for NCC and phospho-NCC was easily detected in the DCT cells of SPAK^{+/+} mice, but was markedly reduced in sections from SPAK[243A/243A] mice (Fig 3C). The reduction was most marked for phospho-NCC, which was almost absent from many sections.

We also analysed whole kidney tissue sections from SPAK^{+/+} and SPAK[243A/243A] mice by microscopy after haematoxylin and eosin and periodic acid Schiff staining. These were found to be indistinguishable (data not shown). Under electron microscopy the renal ultrastructure of SPAK^{+/+} and SPAK[243A/243A] mice were also indistinguishable (Fig S5). In particular, the DCT cells had normal morphology and there was no evidence of systematic differences in height or complexity of basolateral membrane infolding between genotypes as has been reported in NCC^{−/−} mice (Schultheis et al, 1998).

Reduced phosphorylation and expression of NKCC2 in kidney of SPAK knock-in mice

We raised an antibody capable of specifically recognizing NKCC2 (Fig S6A and B). Similar to NCC, immunoblot analysis of cell extracts (Fig 4A) or NKCC2 immunoprecipitates (Fig 4B, upper panel) revealed a moderate reduction in expression of NKCC2 protein in kidney extracts derived from SPAK[243A/243A] mice compared to wild type mice. Quantitative PCR analysis revealed that NKCC2 mRNA levels were similar in the kidney extracts of wild type and SPAK[243A/243A] mice (Fig S4). We observed that one of the NCC phosphospecific antibodies raised recognized human NKCC2 phosphorylated at Thr100 (identical to Thr96 in mouse NKCC2), a major SPAK/OSR1 phosphorylation site (CR, unpublished data). Consistent with this, the antibody recognized wild type human NKCC2, but not mutant NKCC2 [T100A] overexpressed in 293 cells stimulated with hypotonic low-chloride stress in order to activate the SPAK pathway (Fig S6C). Immunoblot analysis of immunoprecipitated NKCC2 revealed significant Thr96 phosphorylation of
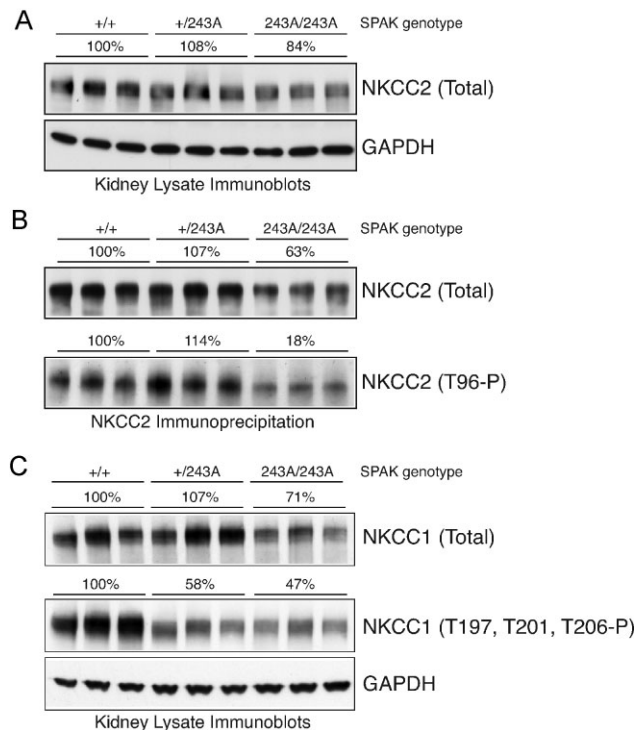
To further localize NCC and phospho-NCC expression, kidneys were microdissected and subjected to immunoblotting. This showed that as expected NCC and phospho-NCC were localized exclusively in DCT tubules. Blots from SPAK[243A/243A] kidneys again showed marked reduction in total NCC and complete loss of staining for phospho-NCC (Fig 3B).

Kidneys from wild type and SPAK[243A/243A] mice were fixed in formalin and sections were stained with NCC total and Thr58 phosphospecific antibodies confirming striking differences

Figure 4. Reduced expression and phosphorylation of NKCC2 and NKCC1 in SPAK[243A/243A] kidney.

A. NKCC2 protein levels in wild type, heterozygous and homozygous knock-in total mouse kidney extract. Kidney extract derived from the indicated mice were subjected to immunoblot analysis with the NKCC2 specific antibody characterized in Fig S6.

B. Analysis of kidney NKCC2 protein levels and phosphorylation in wild type, heterozygous and homozygous knock-in mice following NKCC2 immuno-precipitation. NKCC2 was immunoprecipitated from the indicated kidney extracts and subjected to immunoblot analysis with the total NKCC2 antibody (upper panel) and a phosphospecific antibody recognizing NKCC2 phosphorylated at Thr96 (lower panel), a major SPAK phosphorylation site. Characterization of the NKCC2 T96-P antibody is provided in Fig S6. Each sample is derived from a separate littermate animal.

C. NKCC1 protein levels and phosphorylation in wild type, heterozygous and homozygous knock-in mouse kidney extract. Kidney extract derived from the indicated mice were subjected to immunoblot analysis with the indicated antibodies. Band intensities were quantified using Li-Cor Odyssey and the results are presented relative to the wild type (100%). This study has been repeated over three times each with kidney extracts derived from different animals on each occasion with consistent results.

NKCC2 in extracts derived from wild type or heterozygous SPAK[243A/+] mice which was reduced over five-fold in kidney extracts derived from SPAK[243A/243A] animals (Fig 4B, lower panel).

Reduced phosphorylation and expression of NKCC1 in kidney, but not in other tissues of SPAK knock-in mice

We observed a ~30% reduction in the expression of NKCC1 in kidney extracts derived from SPAK[243A/243A] mice compared to heterozygous or wild type mice (Fig 4C). NKCC1 phosphorylation was analysed employing a previously char-

acterized antibody that recognizes a cluster of three SPAK/OSR1 phosphorylation sites (Thr197/Thr201/Thr206) (Vitari et al, 2006). This revealed a ~50% reduction in NKCC1 phosphorylation in SPAK[243A/243A] kidneys (Fig 4C). We observed in other mouse tissues examined the levels of NKCC1 protein were not markedly reduced in the SPAK[243A/243A] mice compared to wild type (Fig 1A and B, lower panels). Moderate phosphorylation of NKCC1 was detected in lung and testis but this was not reduced in the SPAK knock-in mice (Fig 1A and B, lower panels).

Plasma and urinary electrolyte levels in SPAK243A/243A mice

Electrolytes were measured in venous plasma from mice maintained on a normal Na^+-diet and reported in Table 1. The only significant difference between genotypes was a mild hypomagnesaemia in the SPAK[243A/243A] mice. Urine electrolytes measured in mice on the same normal Na^+-diet showed moderate hypocalciuria; other electrolytes were not significantly different and there was no detectable proteinuria or glycosuria. There was also no difference in plasma aldosterone (Fig 5A) or plasma corticosterone (Fig 5B) between genotypes on a normal Na^+-diet.

To explore a possible role of the renin-angiotensin system (RAS), electrolytes were also measured after 14 days on a Na^+ restricted diet (0.03%). This caused activation of the RAS demonstrated by a substantial rise in plasma aldosterone (Fig 5A) and plasma corticosterone (Fig 5B) in both mouse genotypes. The levels of Na^+ excretion also fell to ~15% of those seen on the normal Na^+-diet (Table 1). Plasma electrolytes showed a relative hypokalaemia in the SPAK[243A/243A] mice after Na^+ restriction (Table 1). As expected the calcium excretion on the low Na^+-diet was low in both mouse genotypes, but not significantly different between genotypes (Schultheis et al, 1998).

To further investigate sodium and potassium handling in the kidney, urinary electrolytes were measured during the transition from a high (3% Na^+) to a low (0.03% Na^+) salt diet (Pradervand et al, 2003). Interestingly, relative to wild-type controls the SPAK[243A/243A] mice showed obvious sodium wasting up to 6h after this transition and potassium wasting between 6 and 24 h (Fig 5C and D). After 4 days the excretion of sodium and potassium reached a steady state and were similar in both genotypes (Fig 5C and D). We also observed that the SPAK[243A/243A] animals expressed ~2-fold higher levels of the three subunits of the epithelial sodium channel (ENaC) in the kidney (Fig 5E), which could compensate for reduced NCC/NKCC2 phosphorylation/activity resulting from loss of SPAK activity.

DISCUSSION

The results presented in this study demonstrate that the effects of the WNK isoforms on blood pressure are likely to be at least in part mediated via activation of SPAK, as knock-in mice expressing a form of SPAK that cannot be activated by the WNK kinases are significantly hypotensive. This indicates that redundancy in the SPAK pathway and other physiological

Table 1. Plasma and urine electrolyte levels

Normal Na$^+$-diet plasma electrolytes	SPAK$^{+/+}$ (mmol/L)	SPAK$^{243A/243A}$ (mmol/L)
Na$^+$	146.90 ± 0.82 ($n = 25$)	146.30 ± 0.80 ($n = 24$)
K$^+$	5.52 ± 0.13 ($n = 22$)	5.33 ± 0.18 ($n = 20$)
Cl$^-$	110.70 ± 0.60 ($n = 25$)	109.10 ± 0.70 ($n = 23$)
Ca^{2+}	2.38 ± 0.01 ($n = 25$)	2.40 ± 0.01 ($n = 23$)
Mg^{2+}	**1.12 ± 0.04 (n = 25)**	**1.01 ± 0.02 (n = 23)***
PO$_4{}^{3-}$	2.12 ± 0.05 ($n = 25$)	2.05 ± 0.09 ($n = 23$)
Low Na$^+$-diet plasma electrolytes	**SPAK$^{+/+}$ (mmol/L)**	**SPAK$^{243A/243A}$ (mmol/L)**
Na$^+$	149.78 ± 1.71 ($n = 9$)	151.45 ± 0.45 ($n = 11$)
K$^+$	**3.49 ± 0.13 (n = 9)**	**3.06 ± 0.09 (n = 11)***
Cl$^-$	109.11 ± 1.49 ($n = 9$)	108.81 ± 0.34 ($n = 11$)
Ca^{2+}	N/D	N/D
Mg^{2+}	0.77 ± 0.03 ($n = 9$)	0.78 ± 0.02 ($n = 12$)
PO$_4{}^{3-}$	**1.92 ± 0.14 (n = 9)**	**2.38 ± 0.11 (n = 12)***
Normal Na$^+$-diet urine electrolytes	**SPAK$^{+/+}$**	**SPAK$^{243A/243A}$**
	(ratio of electrolytes/creatinine)	
Na$^+$	14.33 ± 2.11 ($n = 7$)	15.09 ± 2.45 ($n = 6$)
K$^+$	47.96 ± 4.88 ($n = 7$)	55.03 ± 5.23 ($n = 6$)
Cl$^-$	27.31 ± 4.11 ($n = 7$)	32.20 ± 2.57 ($n = 6$)
Ca^{2+}	**1.37 ± 0.15 (n = 9)**	**0.95 ± 0.07 (n = 9)***
Mg^{2+}	10.40 ± 0.76 ($n = 9$)	10.68 ± 0.61 ($n = 8$)
PO$_4{}^{3-}$	11.24 ± 2.35 ($n = 8$)	17.11 ± 1.42 ($n = 8$)
Low Na$^+$-diet urine electrolytes	**SPAK$^{+/+}$**	**SPAK$^{243A/243A}$**
	(ratio of electrolytes/creatinine)	
Na$^+$	2.33 ± 0.62 ($n = 6$)	2.19 ± 0.58 ($n = 6$)
K$^+$	43.64 ± 3.11 ($n = 6$)	43.64 ± 2.96 ($n = 6$)
Cl$^-$	5.88 ± 0.44 ($n = 6$)	7.19 ± 1.30 ($n = 6$)
Ca^{2+}	0.80 ± 0.16 ($n = 8$)	0.80 ± 0.12 ($n = 10$)
Mg^{2+}	5.49 ± 0.48 ($n = 9$)	5.77 ± 0.39 ($n = 10$)
PO$_4{}^{3-}$	9.44 ± 2.00 ($n = 8$)	8.41 ± 1.52 ($n = 10$)

The indicated mice were fed a normal Na$^+$-diet (0.3%) or subjected to a restricted Na$^+$-diet (0.03%) for 2 weeks. Plasma electrolytes are in mmol/L. Urinary electrolytes are expressed as a ratio of electrolyte concentration to creatinine. Bold type/* indicates $p < 0.05$ versus SPAK$^{+/+}$. N/D indicates not determined due to insufficient sample.

compensatory mechanisms are insufficient to overcome this loss of SPAK kinase activity. Our data suggest that the mechanism by which SPAK regulates blood pressure involves phosphorylation of the crucial renal NCC and NKCC2 ion cotransporters which are targets for the commonly used blood-pressure-lowering thiazide diuretic and loop diuretic drugs. This is based on the finding that SPAK$^{243A/243A}$ animals possess markedly reduced phosphorylation of the NCC and NKCC2 cotransporters. These same residues are phosphorylated by SPAK to promote cotransporter activation leading to enhanced salt reabsorption (Pacheco-Alvarez et al, 2006; Richardson & Alessi, 2008; Richardson et al, 2008). These findings establish that SPAK is a major regulator of the phosphorylation of NCC and NKCC2 in the kidney, reinforcing substantial previous biochemical and overexpression data that indicated NCC/NKCC2 were controlled by a WNK-SPAK signalling pathway (reviewed in Gamba, 2009; Richardson & Alessi, 2008). We also observed reduced phosphorylation of NKCC1 in the kidney of SPAK$^{243A/243A}$ animals (Fig 4C), which is consistent with previous analysis suggesting that SPAK phosphorylated NKCC1 (Gamba, 2009; Richardson & Alessi, 2008; Vitari et al, 2006).

Further work is required to define the role that NKCC1 phosphorylation may play in the kidney.

We also observed that levels of NCC and NKCC2 as well as NKCC1 protein were moderately reduced (30–40%) in the SPAK$^{243A/243A}$ mice under conditions which mRNA levels were unaffected. Further work is required to unravel the mechanism by which SPAK might control the expression of these ion cotransporters, but it is important to note that the distribution of SPAK along the nephron parallels exactly that of NKCC2 and NCC (Fig 1E). It is reported that the WNK-SPAK pathway promotes trafficking of ion cotransporters to the plasma membrane (Cai et al, 2006; Golbang et al, 2005; Wilson et al, 2003; Yang et al, 2003). Reduced phosphorylation of ion cotransporters in SPAK$^{243A/243A}$ animals might suppress trafficking of these proteins to the plasma membrane and thereby promote their degradation perhaps by stimulating translocation to lysosomal or other cellular compartments. It cannot be ruled out that SPAK might regulate expression of ion cotransporters by phosphorylating and suppressing the activity of an E3-ubiquitin ligase that promotes degradation of these ion cotransporters. Thus the reduced blood pressure observed in the
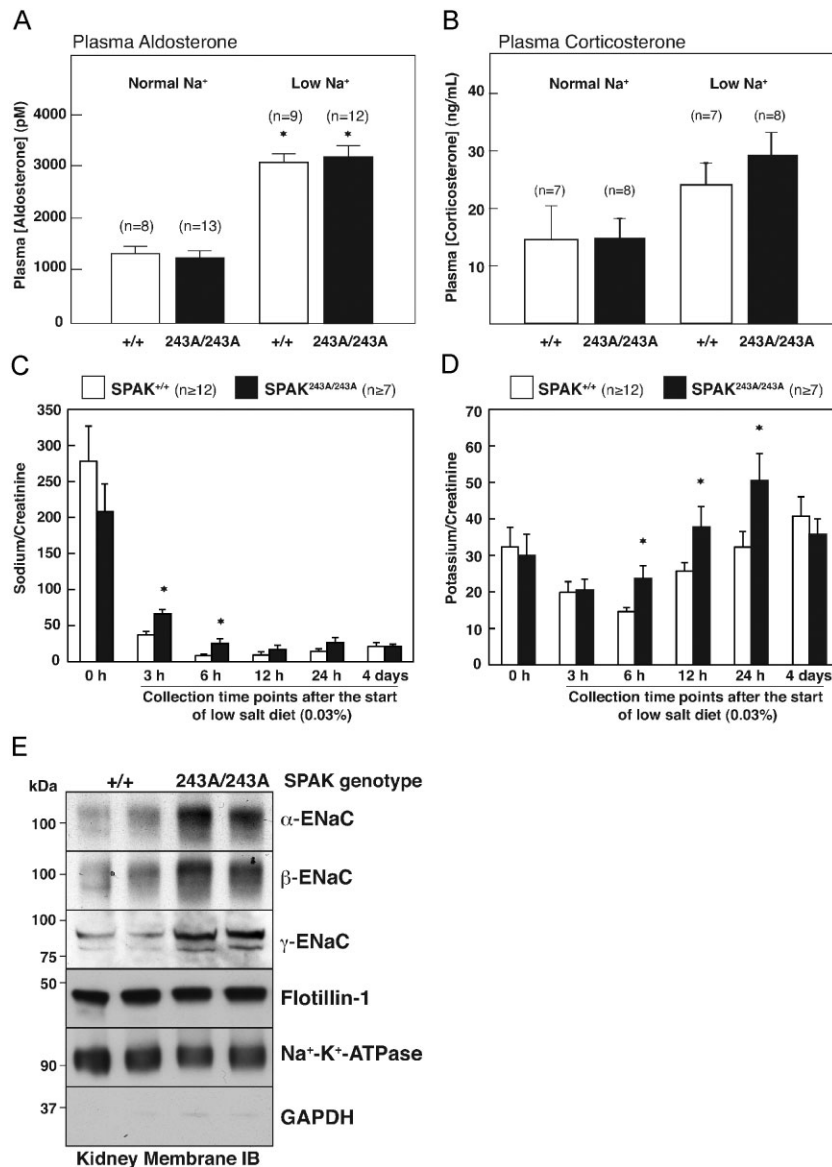
Figure 5. Plasma aldosterone/corticosterone and urine electrolyte levels.

A, B. Plasma aldosterone and corticosterone levels in wild type and knock-in mice. The indicated mice were fed a normal Na^+-diet (0.3%) or subjected to a restricted Na^+-diet (0.03%) for 2 weeks. Plasma aldosterone (A) and corticosterone (B) levels were measured in the indicated mice. $^*p < 0.0001$ versus normal Na^+-diet.

C, D. Urine sodium and potassium levels at indicated time intervals after mice are switched from a high salt diet to a low salt diet. The indicated mice were fed a high salt (3% Na^+) diet for 1 week. Mice were then switched to a restricted low salt (0.03% Na^+)-diet. Urine samples were taken immediately before (0 h) or at the indicated times after switching diets and urinary sodium (C) and potassium (D) levels quantified. $^*p < 0.05$ versus $SPAK^{+/+}$.

E. Expression of ENaC subunits in kidney extracts of wild type and knock-in mice. The indicated membrane preparations (5 μg protein) derived from wild type and $SPAK^{243A/243A}$ mouse kidney were subjected to immunoblot analysis with the specified antibodies. Flotillin and Na-K-ATPase are membrane proteins whilst glyceraldehyde 3-phosphate dehydrogenase (GAPDH) is a cytosolic protein. Similar results were obtained in two separate experiments.

$SPAK^{243A/243A}$ animals is likely to be a result of both reduced phosphorylation and reduced expression of NCC and NKCC2.

A recent genome-wide association study revealed that intronic SNPs within the SPAK gene significantly increased blood pressure in humans (Wang et al, 2009). The mechanism by which these polymorphisms exert their molecular effects requires further investigation, but initial analysis indicated that some of these mutations moderately enhance expression of SPAK in the kidney. If this was the case, overexpression of SPAK in the kidney could increase blood pressure by promoting phosphorylation and expression of NCC and NKCC2. This study together with findings showing that mutations which increase WNK1 expression cause PHAII (Wilson et al, 2001), suggest blood pressure in humans may be sensitive to relatively modest changes in the WNK-SPAK signalling pathway.

The phenotype of hypotension (Fig 2), hypomagnesaemia and hypocalciuria (Table 1) in the $SPAK^{243A/243A}$ knock-in mice has significant parallels with Gitelman's syndrome caused by loss-of-function NCC mutations (Ellison, 2003). In contrast, disruption of the NCC-*SLC12A3* gene in mice only reproduces some aspects of Gitelman's syndrome (Schultheis et al, 1998). A major difference between the NCC and the $SPAK^{243A/243A}$ knock-in mice is that the NCC knock-out animals only display reduced blood pressure when fed a Na^+-restricted diet (Schultheis et al, 1998), in contrast to the $SPAK^{243A/243A}$ mice that are significantly hypotensive on a normal Na^+ diet (Fig 2). Moreover, the mild hypokalaemia observed in the $SPAK^{243A/243A}$ animals on a sodium restricted but potassium replete diet has not been reported in NCC knock-out mice. The salt dependant phenotype of the $SPAK^{243A/243A}$ mouse is supported by the abolition of hypotension following a high salt (3% Na^+) diet (Fig 2E). In the

hypertensive Liddle mice that have mutations in the β subunit of ENaC, no differences in urinary sodium or potassium concentration were seen at a steady state, but differences in renal sodium handling were clearly observed during an acute change in salt intake (Pradervand et al, 2003). Similar observations were made in the SPAK[243A/243A] mice, where transient sodium wasting was observed when switching from high to low salt diet (Fig 5C). We also found that the SPAK[243A/243A] animals expressed ~2-fold higher levels of expression the α, β and γ subunits of the epithelial sodium channel in the kidney (Fig 5E) which might reflect a mechanism to compensate for reduced NCC/NKCC2 activity. Interestingly, hypomorphic WNK4 mice have recently been generated, that also display reduced blood pressure and lower levels of SPAK/OSR1 and NCC phosphorylation (Ohta et al, 2009). The hypomorphic WNK4 mice similar to SPAK[243A/243A] animals possessed increased expression of ENaC in the kidney further suggesting that this is compensation for inhibition of the NCC/NKCC2 (Ohta et al, 2009).

Further work is required to establish the relative contribution of NCC and NKCC2 to renal salt wasting and hypotension seen in the SPAK[243A/243A] animals. Whilst loss-of-function mutation in NKCC2 (Bartter syndrome Type 1) tends to produce more profound hypotension than those with NCC loss-of-function mutations (Gitelman's syndrome), hypocalciuria in the SPAK[243A/243A] mice would favour NCC as the dominant transporter defect. Aldosterone levels are not elevated in SPAK[243A/243A] mice on the normal Na^{+}-diet, but are also frequently normal in Gitelman's patients and also a feature of NCC knock-out mice (Schultheis et al, 1998).

Genetic analysis indicates that SPAK evolved as a result of a gene duplication of OSR1 in evolution of mammals as most non-mammalian species possess only a single isoform bearing greater resemblance to OSR1 than SPAK (Delpire & Gagnon, 2008). SPAK may have evolved to undertake more specialized roles in mammals such as control of NCC and NKCC2 in the kidney. This may also account for the more variable expression of SPAK in different tissues compared with the more ubiquitously expressed OSR1 (Fig 1). The late embryonic lethal phenotype of OSR1[185A/185A] knock-in mice also points towards a more global role for OSR1 that cannot be compensated for by SPAK. It has also been reported that mice generated from a random gene-trap insertion study that lack a portion of the non-catalytic C-terminal domain of OSR1 display late embryonic lethality (Delpire & Gagnon, 2008). Moreover, knock-out of the *Drosophila* orthologue of OSR1, *FRAY*, also results in late lethality in the last larval cycle (Leiserson et al, 2000). Consistent with our findings, a gene-trap mouse lacking the C-terminal portion of SPAK that includes a portion of the kinase catalytic domain is viable (Delpire & Gagnon, 2008). It is also possible that in SPAK[243A/243A] knock-in mice, OSR1 can partly compensate for lack of SPAK activity. For example, the residual phosphorylation of NCC, NKCC2 and NKCC1 observed in the SPAK[243A/243A] knock-in mice may be mediated by OSR1. It has also been elegantly demonstrated that both SPAK and OSR1 contribute to the phosphorylation of NKCC1 in dorsal root ganglion neurons and ablating either of these kinases results in a ~50% reduction in NKCC1 activity (Geng et al, 2009). In other

tissues such as lung and testis, we observed no reduction in NKCC1 phosphorylation or expression in SPAK[243A/243A] mice suggesting that OSR1 principally phosphorylates NKCC1 in these tissues. As the SPAK[243A/243A] mice used in this study ablate SPAK activity in all tissues of the mouse, we cannot rule out that the effects on blood pressure seen in the SPAK knock-in mice could in part result from non-renal (*e.g.* colon, brain, blood vessels) effects. To address this question it would be interesting in future studies to generate a tissue specific nephron knock-in or knock-out of SPAK.

In conclusion, our results establish that SPAK protein kinase is a major regulator of blood pressure. Our data suggest that SPAK regulates blood pressure by controlling the activity as well as expression of the renal sodium cotransporters NCC and NKCC2. The markedly hypotensive phenotype of the SPAK[243A/243A] mice makes SPAK a promising new target for future anti-hypertensive agents and the lack of an overt phenotype of these mice may indicate that SPAK kinase inhibitors may be well tolerated. Owing to the high degree of homology between SPAK and OSR1 it may be challenging to develop drugs that selectively inhibit SPAK. However, even a drug that partially inhibited both SPAK and OSR1 isoforms might reduce phosphorylation and expression of NCC and NKCC2 enough to lower blood pressure without significant adverse effects.

MATERIALS AND METHODS

Antibodies

The following antibodies were raised in sheep and affinity purified on the appropriate antigen: SPAK-mouse antibody (439–453 of mouse SPAK, QSLSVHDSQAQPNAN, S150C), OSR1 mouse antibody (389–408 of mouse OSR1, SAHLPQPAGQMPTQPAQVSL, S149C), SPAK/OSR1 (T-loop) phospho-Thr233/Thr185 antibody (226–238 of human SPAK or residues 178–190 of human OSR1, TRNKVRKpTFVGTP, S204C), SPAK/OSR1 (S-motif) phospho-Ser373/Ser325 antibody (367–379 of human SPAK, RRVPGSpSGHLKT, which is highly similar to residues 319–331 of human OSR1 in which the sequence is RRVPGSpSGRLHKT, S670B), NKCC1 phospho-Thr203, Thr207 and Thr212 (residues 198-217 of human NKCC1, HYYYDpTHTNp-TYYLRpTFGHNT, S763B), NKCC1-total antibody (residues 1-260 of shark NKCC1, S841B), NCC phospho-Thr55 antibody (residues 41–60 of human NCC phosphorylated at Thr55, HPSHLTHSSTFCMRpTFGYNT, S908B), NCC phospho-Thr60 antibody (residues 54–66 of human NCC phosphorylated at Thr60, RTFGYNpTIDVVPT, S995B), NCC phospho-Ser91 antibody (residues 85–97 of human NCC phosphorylated at Ser91, TLADLHpSFLKQEG, S996B), NCC-total antibody (residues 906–925 of human NCC, CHTKRFEDMIAPFRLNDGFKD, S965B), NKCC2-total antibody (residues 1–174 of human NKCC2, S838B) and GST-total antibody (raised against the glutathione S-transferase protein, S902A). A commercial total NCC antibody (AB3553) was purchased from Chemicon International. The anti-GAPDH antibody (ab8245) and the Na^{+}/K^{+}-ATPase (ab8344) were purchased from Abcam. The anti-ERK1/2 antibody (9102) was purchased from Cell Signaling Technology. The antibodies recognizing the α and β subunits of ENaC were a kind gift of S. Wilson (Dundee

The paper explained

PROBLEM:

Hypertension is a largely asymptomatic condition that is a major risk factor for other diseases such as stroke, heart failure and kidney disease. PHAII or Gordon's Syndrome is a rare genetic disorder that is characterized by hypertension and hyperkalemia (high serum potassium). A form of this syndrome is caused by mutations leading to increased expression of the WNK1 protein kinase, but how this is linked to blood pressure is unclear.

RESULTS:

In light of our previous work we asked whether WNK regulated blood pressure via SPAK and generated a genetically modified mouse in which WNK can no longer switch SPAK on. Excitingly, we found that the genetically modified SPAK mice have dramatically reduced blood pressure. In addition, there is reduced activity and expression of the kidney ion cotransporters NCC and NKCC2.

Consistent with these data, plasma and urine electrolyte measurements indicate that the mice display symptoms of salt wasting in particular when under a low-sodium diet.

IMPACT:

The study provides strong genetic evidence that the WNK-SPAK-NCC/NKCC2 signalling network comprises a fundamental regulatory pathway involved in controlling blood pressure. Importantly, our data suggest that drugs that inhibit SPAK kinase would be effective at lowering blood pressure by reducing the activity and expression of NCC and NKCC2. A recent genome-wide association study revealed that intronic SNPs within the human SPAK gene (also known as STK39) could be linked to 20% of the population and lead to increased blood pressure. Together with our results the take home message is that SPAK is a master regulator of blood pressure in humans.

University) and R.C. Boucher (University of North Carolina at Chapel Hill). The antibody recognizing the γ subunit of ENaC was purchased from Sigma (E4902). The antibody recognizing flotillin-1 was purchased from SantaCruz (Sc-25506). Secondary antibodies coupled to horseradish peroxidase used for immunoblotting were obtained from Pierce. Preimmune IgG used in control immunoprecipitation experiments were affinity purified from preimmune serum using protein G-Sepharose.

Buffers

Lysis buffer was 50 mM Tris/HCl, pH 7.5, 1 mM EGTA, 1 mM EDTA, 50 mM sodium fluoride, 5 mM sodium pyrophosphate, 1 mM sodium orthovanadate, 1% (w/v) NP-40, 0.27 M sucrose, 0.1% (v/v) 2-mercaptoethanol, and protease inhibitors (1 tablet per 50 ml). Buffer A was 50 mM Tris/HCl, pH 7.5, 0.1 mM EGTA, and 0.1% (v/v) 2-mercaptoethanol. TBS-Tween buffer (TTBS) was Tris/HCl, pH 7.5, 0.15 M NaCl, and 0.2% (v/v) Tween-20. SDS sample buffer was $1 \times$ NuPAGE LDS sample buffer (Invitrogen), containing 1% (v/v) 2-mercaptoethanol.

Immunoprecipitation and assay of SPAK and OSR1

One milligram of clarified cell lysate was incubated with 5 μg of the SPAK/OSR1 (total) antibody conjugated to 5 μl of protein G-Sepharose and incubated for 2 h at 4°C with gentle agitation. The immunoprecipitates were washed twice with 1 ml of lysis buffer containing 0.5 M NaCl and twice with 1 ml of buffer A. The SPAK/OSR1 immunoprecipitates were assayed with the CATCHtide peptide substrate (RRHYYYDTHTNTYYLRTFGHNTRR) that encompasses the SPAK/OSR1 phosphorylation sites on NKCC1 (Vitari et al, 2006). Assays were set up in a total volume of 50 μl in buffer A containing 10 mM MgCl$_2$, 0.1 mM [γ^{32}P]ATP and 300 μM CATCHtide. After incubation for 30 min at 30°C, the reaction mixture was applied onto P81 phosphocellulose paper, the papers were washed in phosphoric acid, and incorporation of ^{32}P-radioactivity in CATCHtide was quantified by Cerenkov counting.

Generation and genotyping of SPAK and OSR1 knock-in mice

The knock-in mice were generated by TaconicArtemis (http://www.taconic.com/wmspage.cfm?parm1=1453) as described in Supporting Information Fig S1. The knock-in mice were generated and maintained on an inbred C57BL/6J background and confirmed to possess only renin-1 and not renin-2 (Fig S2). Genotyping was performed by PCR using genomic DNA isolated from tails or embryonic membranes. For the SPAK mice, Primer 1 (5′-GTC TAG GAC ATG ATG GTA TGG-3′) and Primer 2 (P2: 5′-CCA ACA TGG GGT ACC AAC AAA TGC-3′) were used to detect the wild type and knock-in alleles as described in Supporting Information Fig 1A and C. The PCR program consisted of 2 min at 95°C; 30 s at 95°C, 1 min at 55°C and 1 min at 72°C: 35 cycles; 5 min at 72°C. For the OSR1 mice, Primer 3 (5′-CGC TGC AGT CTC CTG TCA TCT G-3′) and Primer 4 (5′-CAG AGT GAG GTC TAG GAC AGC CAG G-3′) were used to detect the wild type and knock-in alleles. The PCR program consisted of 4 min at 92°C; 30 s at 92°C, 30 s at 63°C and 1 min at 72°C: 34 cycles.

Animals

Mice were maintained under specific pathogen-free conditions and all procedures were carried out in accordance with the regulations set by the Universities of Cambridge and Dundee, and the United Kingdom Home Office.

Radiotelemetry

Mice were anaesthetized with isoflurane, the left carotid artery was isolated and the tip of the telemeter catheter (transmitter model TA11PA-C10) was inserted in the carotid artery and advanced in the aortic arch, with the telemeter body positioned in a subcutaneous pocket on the right flank. After surgery, each animal was returned to

its home cage and provided with *ad libitum* food and water for the duration of the study. The telemeter signal was processed using RPC-1 receiver, a 20-channel data exchange matrix, APR-1 ambient pressure monitor, and a Data Quest ART Gold 3.0 acquisition system (Data Sciences International, St. Paul, MN, USA). The system was set to sample the mean, systolic, diastolic and pulse pressure, heart rate (HR) and locomotor activity over a 10-sec interval and record their average values. The recording room was maintained at 21–22°C with a 12:12 h light dark cycle (18 to 6 h night and 6–18 h day with 5.30–6 h dawn). The implanted telemeter was active all the time. The data included in the analysis are from three wild type (WT) male mice and four knock-in (KI) male mice that were successfully continuously monitored for at least 10 days (data from two consecutive days were selected for the full scale analysis).

Blood pressure measurement

Mice fed either normal (0.3% sodium), high (3% sodium) or low (0.03% sodium) salt diet for 14 days were anaesthetized using intraperitoneal injection of ketamine (100 μg/g) and midazolam (2 μg/g). Mean arterial blood pressure was measured by cannulation of the right internal carotid artery and recorded and analysed using the Powerlab® data acquisition system and Lab Chart 6® software (AD Instruments Ltd, Oxon, UK).

Statistical analysis

Data are presented as mean ± SEM, with *n* representing the number of analysed mice. Mean values were compared by the Student's *t*-test for paired or unpaired observations were appropriate, using SigmaStat Program (Jandel Scientific, Chicago, IL), or by ANOVA with *post hoc* testing using version 15 of SPSS software. $p < 0.05$ was considered statistically significant.

Analysis of plasma and urine

Blood was collected from either the tail vein of awake mice using Microvette® CB300 tubes (Sarstedt Ltd, Leicester, UK) or from a carotid artery cannulation in anaesthetized mice. Plasma was recovered by centrifugation. Spot urine was collected from awake mice following spontaneous micturition on handling over a sheet of Saran® wrap. Samples were collected from mice either on a normal Na$^+$-diet (0.3% Na, 0.69% K, 0.22% Mg, 0.74% Ca, 0.63% P, SDS diet # 801730, Witham Essex, UK) or after 14 days of a low Na$^+$ diet (total Na$^+$ reduced to 0.03%). To investigate the transition between high and low salt diets, mice were fed a high Na$^+$ (3%) diet for 10 days and urine collected. Mice were then change to a low Na$^+$ (0.03%) diet and urine collected at 3, 6, 12, 24 h and 4 days. Electrolyte analysis was performed using the Dade-Behring Dimension RXL analyser. Plasma aldosterone was measured using the DPC Coat-A-Count® radioimmunoassay (DPC, Llanberis, Caernarfon, Gwynedd) and urinary protein and glucose analysis performed using Multistix® (Bayer HealthCare, Newbury, UK). Plasma corticosterone was measured using the corticosterone EIA kit from immunodiagnosticsystems (catalogue number AC-14F1, Boldon, UK). All studies were performed between 0800 and 1200 h which is the nadir of corticosterone release in rodents (Cheifetz, 1971).

Microdissection of tubular segments from the kidney

This followed the previously published method (Michlig et al, 2004). Briefly, isolated tubules were obtained by microdissection of the left

kidney perfused with 40 μg/ml Liberase Blendzyme 2 (Roche Applied Science) dissolved in DMEM/F-12 (1:1) medium (21041 medium, Invitrogen). Thin pyramids cut along the corticomedullary axis were incubated at 37°C for 40 min in aerated DMEM/F-12 (1:1) medium containing 40 μg/ml Liberase. Microdissection was performed in ice-cold DMEM/F-12 (1:1) and the following structures were isolated: glomerulus (Glom), proximal convoluted tubule (PCT), proximal straight tubule (PST), MTAL, CTAL, DCT, connecting tubule (CNT), cortical collecting duct (CCD) and outer medullary collecting duct (OMCD). Tubular length was measured with an ocular micrometer, and pools of 10–20 microdissected tubules with the total tubular length of ∼10 mm/pool were transferred in 5 μl of DMEM/F-12 (1:1) medium into 0.5 ml of Eppendorf tubes.

Mouse kidney Immunocytochemistry

Paraffin embedded renal tissue was blocked with 0.3% Hydrogen Peroxide and 10% BSA/PBS before incubation with the primary antibody. Biotinylated secondary antibody was applied followed by staining with Vectastain® ABC reagent (Vector Labs Ltd, Peterborough, UK) for 30 min according to the manufacturer's protocol. Liquid Diaminobenzidine (DAKO Ltd, Ely, UK) was used as a chromogenic agent for 5 min and sections were counterstained with Mayer's haematoxylin. Sections known to stain positively were included in each batch and negative controls were prepared by replacing the primary antibody with TBS buffer.

In the Supporting Information, further details of materials, general methods, plasmids, cell culture and transfections, expression and purification of SPAK and OSR1 in *E. coli*, immunoblotting, mass spectrometry analysis, electron microscopy and real-time quantitative PCR are provided.

The authors declare that they have no conflict of interest.

For more information

OMIM, Online Mendelian Inheritance in Man
Pseudohypoaldosteronism, type II; pha2
http://www.ncbi.nlm.nih.gov/entrez/dispomim.cgi?id=145260

Accompanying Closeup:
DOI 10.1002/emmm.200900059

References

Cai H, Cebotaru V, Wang YH, Zhang XM, Cebotaru L, Guggino SE, Guggino WB (2006) WNK4 kinase regulates surface expression of the human sodium chloride cotransporter in mammalian cells. Kidney Int 69: 2162-2170

Cheifetz PN (1971) The daily rhythm of the secretion of corticotrophin and corticosterone in rats and mice. J Endocrinol 49: xi-xii

Delpire E, Gagnon KB (2008) SPAK and OSR1: STE20 kinases involved in the regulation of ion homoeostasis and volum control in mammalian cells. Biochem J 409: 321-331

Ellison DH (2003) The thiazide-sensitive na-cl cotransporter and human disease: reemergence of an old player. J Am Soc Nephrol 14: 538-540

Flatman PW (2008) Cotransporters, WNKs and hypertension: an update. Curr Opin Nephrol Hypertens 17: 186-192

Gamba G (2009) The Thiazide-sensitive Na^+:Cl^- Cotransporter: molecular biology, functional properties, and regulation by WNKs. Am J Physiol Renal Physiol 297: F838-848

Geng Y, Hoke A, Delpire E (2009) The Ste20 kinases Ste20-related proline-alanine-rich kinase and oxidative-stress response 1 regulate NKCC1 function in sensory neurons. J Biol Chem 284: 14020-14028

Golbang AP, Murthy M, Hamad A, Liu CH, Cope G, Van't Hoff W, Cuthbert A, O'Shaughnessy KM (2005) A new kindred with pseudohypoaldosteronism type II and a novel mutation (564D > H) in the acidic motif of the WNK4 gene. Hypertension 46: 295-300

Huang CL, Cha SK, Wang HR, Xie J, Cobb MH (2007) WNKs: protein kinases with a unique kinase domain. Exp Mol Med 39: 565-573

Kahle KT, Ring AM, Lifton RP (2008) Molecular physiology of the WNK kinases. Annu Rev Physiol 70: 329-355

Ko B, Hoover RS (2009) Molecular physiology of the thiazide-sensitive sodium-chloride cotransporter. Curr Opin Nephrol Hypertens 18: 421-427

Lee BH, Chen W, Stippec S, Cobb MH (2007) Biological cross-talk between WNK1 and the transforming growth factor beta-Smad signaling pathway. J Biol Chem 282: 17985-17996

Leiserson WM, Harkins EW, Keshishian H (2000) Fray, a Drosophila serine/threonine kinase homologous to mammalian PASK, is required for axonal ensheathment. Neuron 28: 793-806

Lenertz LY, Lee BH, Min X, Xu BE, Wedin K, Earnest S, Goldsmith EJ, Cobb MH (2005) Properties of WNK1 and implications for other family members. J Biol Chem 280: 26653-26658

Michlig S, Mercier A, Doucet A, Schild L, Horisberger JD, Rossier BC, Firsov D (2004) ERK1/2 controls Na,K-ATPase activity and transepithelial sodium transport in the principal cell of the cortical collecting duct of the mouse kidney. J Biol Chem 279: 51002-51012

Ohta A, Rai T, Yui N, Chiga M, Yang SS, Lin SH, Sohara E, Sasaki S, Uchida S (2009) Targeted disruption of the Wnk4 gene decreases phosphorylation of Na-Cl cotransporter, increases Na excretion and lowers blood pressure. Hum Mol Genet 18: 3978-3986

Pacheco-Alvarez D, Cristobal PS, Meade P, Moreno E, Vazquez N, Munoz E, Diaz A, Juarez ME, Gimenez I, Gamba G (2006) The Na^+:Cl^- cotransporter is activated and phosphorylated at the amino-terminal domain upon intracellular chloride depletion. J Biol Chem 281: 28755-28763

Pradervand S, Vandewalle A, Bens M, Gautschi I, Loffing J, Hummler E, Schild L, Rossier BC (2003) Dysfunction of the epithelial sodium channel expressed in the kidney of a mouse model for Liddle syndrome. J Am Soc Nephrol 14: 2219-2228

Pradervand S, Wang Q, Burnier M, Beermann F, Horisberger JD, Hummler E, Rossier BC (1999) A mouse model for Liddle's syndrome. J Am Soc Nephrol 10: 2527-2533

Richardson C, Alessi DR (2008) The regulation of salt transport and blood pressure by the WNK-SPAK/OSR1 signalling pathway. J Cell Sci 121: 3293-3304

Richardson C, Rafiqi FH, Karlsson HK, Moleleki N, Vandewalle A, Campbell DG, Morrice NA, Alessi DR (2008) Activation of the thiazide-sensitive Na^+-Cl^- cotransporter by the WNK-regulated kinases SPAK and OSR1. J Cell Sci 121: 675-684

Schultheis PJ, Lorenz JN, Meneton P, Nieman ML, Riddle TM, Flagella M, Duffy JJ, Doetschman T, Miller ML, Shull GE (1998) Phenotype resembling Gitelman's syndrome in mice lacking the apical Na^+-Cl^- cotransporter of the distal convoluted tubule. J Biol Chem 273: 29150-29155

Shao L, Ren H, Wang W, Zhang W, Feng X, Li X, Chen N (2008) Novel SLC12A3 Mutations in Chinese Patients with Gitelman's Syndrome. Nephron Physiol 108: 29-36

Sigmund CD, Gross KW (1991) Structure, expression, and regulation of the murine renin genes. Hypertension 18: 446-457

Simon DB, Karet FE, Hamdan JM, DiPietro A, Sanjad SA, Lifton RP (1996a) Bartter's syndrome hypokalaemic alkalosis with hypercalciuria (is) caused by mutations in the Na-K-2Cl cotransporter NKCC2. Nat Genet 13: 183-188

Simon DB, Nelson-Williams C, Bia MJ, Ellison D, Karet FE, Molina AM, Vaara I, Iwata F, Cushner HM, Koolen M, et al (1996b) Gitelman's variant of Bartter's syndrome, inherited hypokalaemic alkalosis, is caused by mutations in the thiazide-sensitive Na-Cl cotransporter. Nat Genet 12: 24-30

Vitari AC, Deak M, Morrice NA, Alessi DR (2005) The WNK1 and WNK4 protein kinases that are mutated in Gordon's hypertension syndrome phosphorylate and activate SPAK and OSR1 protein kinases. Biochem J 391: 17-24

Vitari AC, Thastrup J, Rafiqi FH, Deak M, Morrice NA, Karlsson HK, Alessi DR (2006) Functional interactions of the SPAK/OSR1 kinases with their upstream activator WNK1 and downstream substrate NKCC1. Biochem J 397: 223-231

Wang Y, O'Connell JR, McArdle PF, Wade JB, Dorff SE, Shah SJ, Shi X, Pan L, Rampersaud E, Shen H, et al (2009) From the Cover: Whole-genome association study identifies STK39 as a hypertension susceptibility gene. Proc Natl Acad Sci USA 106: 226-231

Wilson FH, Disse-Nicodeme S, Choate KA, Ishikawa K, Nelson-Williams C, Desitter I, Gunel M, Milford DV, Lipkin GW, Achard JM, *et al* (2001) Human hypertension caused by mutations in WNK kinases. Science 293: 1107-1112

Wilson FH, Kahle KT, Sabath E, Lalioti MD, Rapson AK, Hoover RS, Hebert SC, Gamba G, Lifton RP (2003) Molecular pathogenesis of inherited hypertension with hyperkalemia: the Na-Cl cotransporter is inhibited by wild-type but not mutant WNK4. Proc Natl Acad Sci USA 100: 680-684

Xu BE, Stippec S, Lenertz L, Lee BH, Zhang W, Lee YK, Cobb MH (2004) WNK1 activates ERK5 by an MEKK2/3-dependent mechanism. J Biol Chem 279: 7826-7831

Yan Y, Nguyen H, Dalmasso G, Sitaraman SV, Merlin D (2007) Cloning and characterization of a new intestinal inflammation-associated colonic epithelial Ste20-related protein kinase isoform. Biochim Biophys Acta 1769: 106-116

Yang CL, Angell J, Mitchell R, Ellison DH (2003) WNK kinases regulate thiazide-sensitive Na-Cl cotransport. J Clin Invest 111: 1039-1045

Zagorska A, Pozo-Guisado E, Boudeau J, Vitari AC, Rafiqi FH, Thastrup J, Deak M, Campbell DG, Morrice NA, Prescott AR, *et al* (2007) Regulation of activity and localization of the WNK1 protein kinase by hyperosmotic stress. J Cell Biol 176: 89-100

Zambrowicz BP, Abuin A, Ramirez-Solis R, Richter LJ, Piggott J, BeltrandelRio H, Buxton EC, Edwards J, Finch RA, Friddle CJ, *et al* (2003) Wnk1 kinase deficiency lowers blood pressure in mice: a gene-trap screen to identify potential targets for therapeutic intervention. Proc Natl Acad Sci USA 100: 14109-14114